Spontaneous localized fluid release on swelling fibres

Pierre van De Velde, Julien Dervaux, Suzie Protière, Camille Duprat

Check for updates

Spontaneous localized fluid release on swelling fibres †

Pierre Van de Velde, ⓘ *a Julien Dervaux, b Suzie Protière‡*c and
Camille Duprat ⓘ ‡a

When immersed into a favourable solvent, many fibres, in particular vegetable, wood or animal fibres, will absorb liquid and swell. When a single drop of solvent is deposited, the fibre first locally swells at the drop position, then the liquid slowly diffuses within the fibre. We study the absorption dynamics of several drops placed on a fibre of fixed length. We show that during absorption, there is a swelling-induced global change in the tension of the fibre. If the drops are close enough to one another, this change induces the release of fluid out of the fibre (i.e. deswelling) in previously fluid-saturated regions. We identify the mechanisms underlying this transient localized fluid release, and identify the conditions for which it occurs in order to build a phase diagram as a function of the drops volume and distance, both experimentally and numerically using a linear poroelastic model.

The swelling of fibrous materials is observed in many natural systems such as paper, textile or architectural constructions. Indeed, in many industrial processes, a solvent will be imbibed by a complex network of fibres. The liquid front dynamics can then be linked to the orientation of the fibres [1–3] and elastic fibres are even found to collapse when a finite amount of liquid is placed between them.[4] Moreover, in most fibrous materials, fibres are under tension as they are held together by forming a tight network that can be knitted, woven or nonwoven and the volumetric growth induced by the swelling should greatly affect its mechanical properties. We investigate the swelling of model gel fibres, for which we can benefit from the extensive work from the last 70 years [5] where the swelling of a gel was studied to understand the mechanics of growth and pattern formation in soft matter. [6,7]

The specific fibre geometry will promote a localized swelling and makes the swelling dynamics highly dependent on the solvents volume. [8] Indeed, the fibre geometry can keep finite volumes of wetting liquids, which would normally spread, into a compact shape. [9,10] When the swelling is localized, morphological changes can be triggered. [11,12] Shape changes can also be caused by the solvents motion on swellable structures either via evaporation [13] or capillarity. [14] By placing droplets of solvent on an elastomeric fibre, we show that the localized swelling can induce the release of liquid from the fibre which will lead to liquid motion along the fibres surface, a phenomenon that has not been explored yet. In this paper, we explain how the tension within the fibres plays a crucial role in the swelling dynamics of such systems and induces the mobility of the fluid. The effect of mechanical stresses on the swelling has been explored before. As the solvent penetrates the fiber, the polymer expands. The equilibrium shapes and swelling dynamics are governed by the interplay between the osmotic pressure sucking the solvent molecules into the material and the elastic deformations of the material which tend to resist the swelling. [15–17,22] Most previous studies focus on immersed objects. [18–20] In this paper, we specifically study the simultaneous absorption of two drops placed on the same fibre of fixed length. The absorption of each drop influences the other by slowing down the absorption. In extreme cases where the drops are close enough together the swelling-induced compression of the fibre causes a localized fluid release. Using a linear poroelastic model we then explain how this phenomenon occurs depending on the characteristics of the system.

1 Experiments

We mold elastomeric fibres using polyvinylsiloxane (PVS) of initial radius $R = 250$ μm, Young's modulus $E = 0.9$ MPa and length $2L_0 = 3$ cm. To mimic the situation in a woven textile, the fibres are stretched horizontally to a length $2L = 4$ cm and attached to a clamp on one side and to a force sensor (Futek Miniature S-Beam Jr. Load Cell 2.0) measuring the fibre tension on the other side. We will see that the tension has an influence on the fluid absorption. The length of the fibre is fixed once

a LadHyX, Ecole Polytechnique, UMR 7646, Palaiseau, France
b Matiere et Systèmes Complexes, CNRS, UMR 7057, Université de Paris, Paris, France
c Institut Jean Le Rond d'Alembert, Sorbonne Université CNRS, UMR 7190, Paris, France. E-mail: protiere@ida.upmc.fr

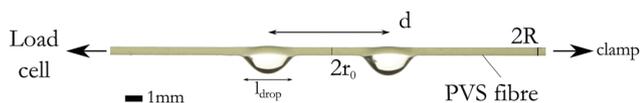‡ These authors contributed equally to this work.

Fig. 1 Experimental setup and notations used to describe two drops of solvent on a swellable fibre. The center of the fibre corresponds to $z = 0$. The drops are placed at $\pm d_0/2$ from the center.

and for all. Using a micro-pipette, we place one or two droplet(s) of silicone oil (viscosity $\eta = 5.4$ mPa s) ofinitial volume V on the fibre at $t = 0$ (Fig. 1). The same batch of silicone oil is used for all experiments. Due to its strong affinity with the polymer, the silicone oil is absorbed by the fibre causing it to swell. For one drop, placed at the center of the fibre (Fig. 2A), the apparent drop volume decreases over time until the drop is fully absorbed. The fibre first swells below the drop and in its immediate vicinity until it reaches an apparent maximal radius R_{max}. We define the swelling ratio λ such that:

$$\lambda = \frac{R_{max}}{R} \tag{1}$$

The fluid then continues to diffuse to each side of the drop until it is completely absorbed. The final result is a swollen region of the fibre of a given length that will then slowly relax until the fibre is uniform over its whole length (not shown here). This absorption dynamics has been described in a previous study.[8] We introduce a lengthscale $L_{swollen}$ which is an estimate for the length of the swollen region. This length is the minimal final length offibre necessary to absorb a drop of initial volume V_0. It is a good approximation for the length of the swollen region shown in Fig. 2A.

$$L_{swollen} = \frac{V_0}{\pi R^2 (\lambda^2 - 1)}. \tag{2}$$

Simultaneously, we monitor the tension in the fibre with the force sensor. The initial stretch $\varepsilon = \frac{L \ominus \frac{1}{4} 0 \vdash}{L_0} = 33\%$ corresponds to a tension of $T = E \varepsilon \pi R^2 = 37.2$ mN. As the drop is absorbed, the fibre swells both radially and axially which causes the strain, therefore the tension within the fibre, to decrease over the course of the experiment. The evolution of the tension for drops of different initial volumes is plotted in Fig. 2B. Initially, the tension in the fibre rapidly decreases as solvent is quickly absorbed below the drop. Once the fibre is locally saturated with solvent below the drop, the absorption – decrease in tension – slows down as diffusion to the sides of the drops is slower than the initial absorption since it now occurs over a longer length and in a single dimension. The dynamic of the decrease in tension is directly correlated to the absorption dynamics (see ESI † Fig. 1). The final tension, measured once the drop is fully absorbed, decreases with the initial drop volume. Some softening of the material can be observed when performing flexion experiments on dry and swollen fibres ($E_{swollen} \subset E_{dry}/2$). Nonetheless its exact effect on the fibre tension is non-trivial as the geometry is also modified by the swelling. The decrease in tension is mainly due to the reduction of stretch via swelling in the axial direction, and we consider E to be constant in all that follows.

We now place two drops symmetrically such that $z = \pm\frac{d_0}{2}$ as shown in Fig. 1. For simplicity, we set the volume of each drop to V = 2 mL unless otherwise specified. For a drop of volume $V_0 = 2$ mL, $L_{swollen} = 11 \pm 1$ mm. Again, we observe the evolution of the drops and track the tension over time. Depending on the initial distance d_0 between the drops, we notice different behaviors. If the drops are placed far from one another, i.e. $d_0 \subset L_{swollen}$, as in Fig. 2C, the absorption dynamics is similar to the single drop case: a rapid initial absorption is followed by a slower diffusion to the sides of the drops until all the oil is
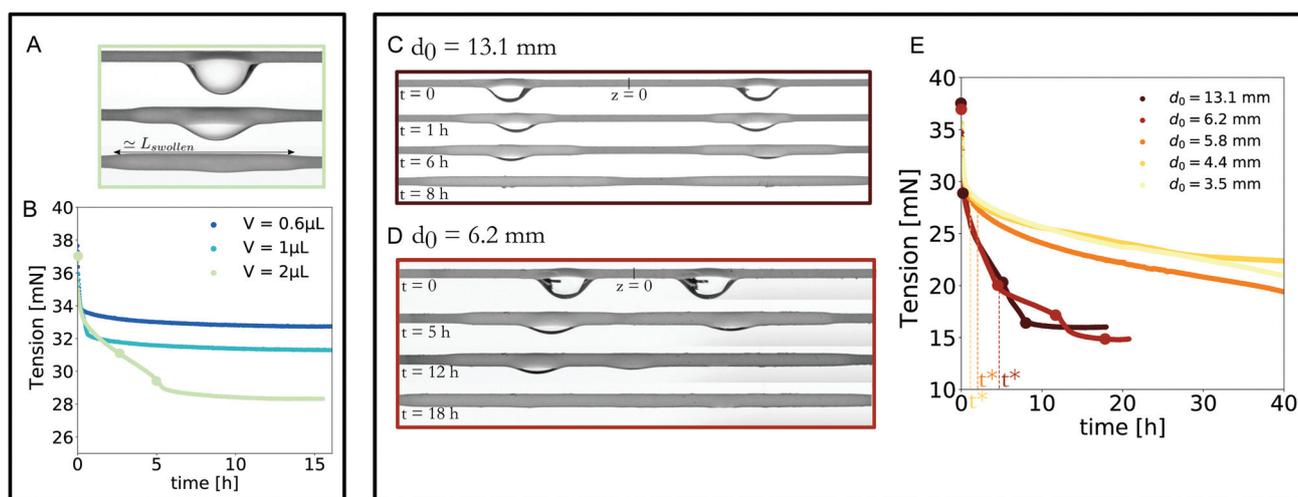

Fig. 2 Experiments: tension decrease during the absorption of one or two drops. (A) Pictures of a single drop on a swellable fibre over time. The radius of the fibre increases as the fluid is absorbed by the polymeric network. Dots on the curve in panel (B) correspond to the pictures. (B) Tension in the fibre during the absorption of a single drop of silicone oil of various initial volumes. (C) Two drops placed at a large initial distance are absorbed with similar dynamics to the single drop experiment. (D) Fluid deswelling between the two initial drops leads to the formation of a third drop that interacts with the initial drops causing them to move. (E) Tension in the fibre during the absorption of two drops ofinitial volumes 2 mL each placed at different initial distances d_0.

absorbed. We end up with two distinct swollen regions that further relax slowly over time. When the initial distance between the two drops is reduced, i.e. $d_0 \approx L_{swollen}$, as in Fig. 2D, the drops interact while swelling the fibre: the drops are absorbed and the two swollen regions of the fibre merge before all the oil is absorbed. We call R_0 the radius at $z = 0$, the center between the two drops. At this position the fibre swells until its radius reaches R_{max}. We define t^* the time at which the fibre is saturated with fluid at $z = 0$, i.e. $R_0(t^*) = R_{max}$. At time t^*, once the portion of the fibre between the drops is fully saturated with liquid, we observe that some fluid is expelled out of the fibre, leading to the formation of a third drop (Fig. 2D $t = 12H$ and Movie S1, ESI †). We call this spontaneous phenomenon "localized deswelling". The released volume is highly variable and depends on the distance between the drops as well as their initial volume. In many cases, the newly formed drop will interact with the initial drops, leading to the spontaneous motions of the drops (Movies S1 and S2, ESI †). These motions modify the drop positions on the fibre and highly influence the absorption dynamics. Indeed, drops usually move towards the center, i.e. away from dry (unswollen) regions, leading to a slow down of the absorption. When the drops are closer, i.e. d_0 is of order of a drop length, the expelled fluid directly interacts with the two initial drops, i.e. forms a liquid bridge between the drops, leading to their spontaneous coalescence (Movie S2, ESI †).

Fig. 2E shows the measured tension for two drops of volume 2 mL each at different initial distances. For experiments where no deswelling is observed (e.g. when $d_0 = 13.1$ mm $\approx 4 L_{swollen}$) the evolution of the tension is similar to the single drop case. The decrease of tension depends solely on the total amount of fluid absorbed through the final swollen length of the fibre and does not depend on the initial distance between drops, nor the number of drops (i.e. a single drop of volume V or two well separated drops of volume $V/2$ lead to the same decrease in tension). At long times, the same tension is reached in all experiments (around 15 mN). Variations in the final tension can be attributed to errors on the initial drop volume (± 0.1 mL), the initial tension as well as slight errors in alignment when attaching the fibre to the sensor.

As the drops are placed closer, the absorption dynamic changes radically. Once the fibre radius has reached R_{max} at $z = 0$, we observe a slowing down of the decrease in tension. The diffusion gets hindered towards the center as the solvent concentration increases in that region. The solvent can only diffuse to one side of each drop and the absorption is thus much slower than the case without any interactions. This effect is stronger if the drops are closer together as the center will be saturated with fluid at earlier times. Indeed t^* depends on the initial distance d_0 and may not be reached if the drops are too far apart or if the volume of the drops is too small (Fig. 2E). When localized deswelling occurs, the dynamics of the absorption is impacted as the position of the drops and thus the distribution of the solvent sources on the fibre are completely modified. In particular, when the drops coalesce ($d_0 = 3.5$ and 4.4 mm in, Fig. 2E), only one source of solvent remains, slowing

down the absorption even more. The total absorption time ranges from 6 hours without interactions to over 60 hours for two drops that coalesce.

To the best of our knowledge, spontaneous localized deswelling has not been reported in the literature. An explanation for the fluid release arises from the properties of the elastomer. Indeed, the quantity of fluid that a gel is able to absorb depends on the stress in the material. [21–24] Stretched fibres can absorb more fluid than unstretched fibres. Intuitively, one might observe that a compression of the fibre will reduce its capacity to absorb fluid as less space is available for the fluid molecules. In our case, as the tension in the fibre is continuously decreasing over the course of the experiment, the equilibrium solvent concentration and thus the maximal radius R_{max} of the fibre decreases over the course of the experiment. At $t = t^*$ the fibre radius at the center is equal to a maximal radius corresponding to the tension $T(t^*)$. From there, as the fluid continues to diffuse to the sides of the drops, the tension further decreases which lowers R_{max}. There is then an excess of fluid in the region between the drops. The fluid is "squeezed" and has to escape. We believe it is more favorable to escape the fibre via localized deswelling than to migrate through the fibre towards regions of lower fluid concentration, which are located at a much larger distance than the free surface.

In the next sections, we show how we can predict the initial drop distances and volumes at which deswelling occurs when varying the system's parameters. We propose a model using linear poroelasticity, and first rationalize our explanation of the spontaneous deswelling process before giving more details on the absorption dynamics and the evolution of the fibre radius and tension.

2 Model

We model our experiment in the framework of linear poroelasticity. [25,26] We consider a poroelastic gel-like material that is not subjected to any mechanical load in its reference state. The initial concentration of solvent molecules in the poroelastic material is homogeneous and given by c_0 while the chemical potential is μ_0. In the deformed state, the system is described by the solvent concentration c, chemical potential μ and displacement field u. In response to the application of an external force, or when the poroelastic material is brought into contact with a reservoir of solvent molecules at a chemical potential different from μ_0, the solvent is not in diffusive equilibrium and will migrate, causing the material to either swell of deswell. To simplify our problem, we assume the concentration in the fibre to be homogeneous in the radial direction, which is true at large timescales for which the fibre radius becomes small compared to the length-scale over which the fluid diffuses. Assuming molecular incompressibility, we can write the following equations (ESI † for full development):

$$u_r(r, z, t) = r \frac{2(c - c_0)GO - s_{zz}(t)}{6G} \tag{3}$$

$$\frac{\partial \bar{u}_z}{\partial z} = \frac{(\bar{c} - c_0)\Omega G - s_{zz}(t)}{6G} \qquad (4)$$

$$\bar{\mu}(z,t) = \mu_0 + \frac{2G\Omega^2(1+n)}{3(1-2n)}(\bar{c} - c_0) - \frac{\Omega s_{zz}(t)}{3} \qquad (5)$$

where G is the bulk modulus of the fibre, Ω is the molar volume of the solvent and n is the poroelastic Poisson ratio that accounts for the ability of a polymer to swell by absorbing solvent. Finding its value experimentally is difficult.[26] We thus assume a value of $n = 1/3$ as used in most studies in the literature.[26] s_{zz} is the stress in the axial direction. The swelling driving pressure is an osmotic pressure,[15] $P_{mix} \sim \frac{RT}{\Omega} \sim 10^6$ Pa, and the pore pressure is of order $B \sim G \sim 3 \times 10^5$ Pa, which is much higher than the Laplace pressure inside the drop $P_{laplace} \sim \frac{\gamma}{H} \sim 10$ Pa, such that we do not take into account surface tension effects in this modelling.

The dimension of these equations is reduced by integrating over the radius of the fibre the continuity equation describing the conservation of the number of solvent molecules in the presence of source. This leads to the following equation describing the spatio-temporal distribution of the solvent in the fibre:

$$\frac{\partial \bar{c}}{\partial t} = D\frac{\partial^2 \bar{c}}{\partial z^2} + \frac{2D}{Rh}(c_{max}(t) - \bar{c})\mathbb{1}_d(z,t) \qquad (6)$$

The distribution $\mathbb{1}_d(z,t)$ is indicative of the drops: it is a distribution whose value is 1 if there is a drop on the fibre at position z and time t and zero otherwise. Eqn (6) is essentially a diffusion equation with a non-trivial source term at the position of the drops. This source term arises from the difference in chemical potential in the fibre below the drop and in the drop itself. In eqn (6), it appears as a source term proportional to the difference between the concentration in the fibre $\bar{c}$ and a normalized, stress-dependent, concentration in $c_{max}(t)$. h is a length (presumably microscopic) that characterizes the interface such that the quantity $k/2h$ is a surface permeability. The competition between h (driving the intensity of the source) and D (driving the speed at which the fluid moves away from the sources once in the fibre) governs the overall dynamics of the absorption. $c_{max}(t)$ is the concentration that a homogeneously swollen fibre would reach when held at a given tension corresponding to a stress s_{zz} in contact with a fluid reservoir at chemical potential μ_b. In our experiment the tension is not constant. Since the length of the fibre is maintained constant, the stress s_{zz} in the fibre only depends on the total amount of absorbed fluid. The value of $c_{max}(t)$ is given by:

$$c_{max}(t) = c_0 + \frac{3(1-2n)}{2G\Omega^2(1+n)}\left(\mu_b - \mu_0 + \frac{\Omega s_{zz}(t)}{3}\right) \qquad (7)$$

We recover the fact that there is no swelling ($i.e.\ c_{max} = c_0$ at all time) if the Poisson ratio is equal to 1/2. When the chemical potential of the solvent molecules in the drop is higher than that of the fibre ($\mu_b > \mu_0$), the fibre swells. It can be seen with eqn (7) that when no change on the chemical potential ($\mu_b = \mu_0$)

and on the stress ($s_{zz} = 0$) are exerted on the fibre, then no swelling or deswelling occurs ($c_{max} = c_0$) as mentioned previously. Interestingly, the tension in the fibre also affects the equilibrium concentration: when the tension increases, the fibre absorbs more liquid. The effective diffusion coefficient D appearing in (6) is $D = \frac{2kG(1+n)}{3Z(1-2n)}$. Finally, we need an equation for the tension in the fibre. This equation is provided by the boundary condition at the end of the fibre. Here we focus on a fibre that is initially stretched and whose ends are subsequently held fixed. We can deduce the lengthwise stress by integrating the displacement and obtain an expression depending on the total absorbed fluid volume:

$$s_{zz}(t) = 3Ge - \frac{G\Omega}{2L}\int_{-L}^{L}(\bar{c} - c_0)dz \qquad (8)$$

The dependence of the equilibrium concentration on the tension (eqn (7) and (8)) is one of the key ingredients to explain the deswelling, as may be illustrated by the following experiment (Movie S3, ESI †): we saturate a fibre with fluid at high tension; when the tension in the fibre is suddenly released, fluid is expelled from the swollen fibre and forms multiple visible drops at the surface of the fibre. Once combined, eqn (6)–(8) form an integrodifferential equation. The fluid diffusion, which is due to local effects, is affected by global constraints (constant length of the fibre) which directly modifies the maximal fluid concentration in the fibre. These global constraints on the fibre are responsible for the localized deswelling as will be described in the next section.

3 Results

3.1 Tension and deswelling

Eqn (6) is solved using a finite difference scheme of order 1. Finding an accurate value for the diffusion coefficient D is difficult. To our knowledge, there is no precise value in the literature for our material: the value of D is highly dependent on the system's geometry.[19,27] We choose $D = 0.93 \times 10^{-10}$ m^2 s^{-1} which corresponds to a value fitted with an empirical model from measurements of the swelling dynamics of a fibre of the same elastomer fully immersed in the same solvent.[8] This value of D corresponds to a permeability $k = \eta D/E \sim 10^{-18}$ m^2 which is coherent with previously reported results.[11,28] The dynamics of the drop absorption being dependent the value of D, we are aware that this might be a source of inaccuracy in the model. The value of D highly depends on the oil viscosity. In fact $D \sim 1/Z$.[8,29] We have observed all behaviours described above with another oil ($Z = 2.3$ mPa s).

The other unknown in our model is the value of h. Fig. 3A shows how sensitive our modeling is to the choice of h. Comparing the simulation for the single drop experiment with our model, we chose $h = 250$ μm which is close to the radius of the fibre and provides the best fit to our experiments (3B). The grey region shows the range of values predicted when varying h. For one drop (Fig. 3B) we are able to accurately reproduce the
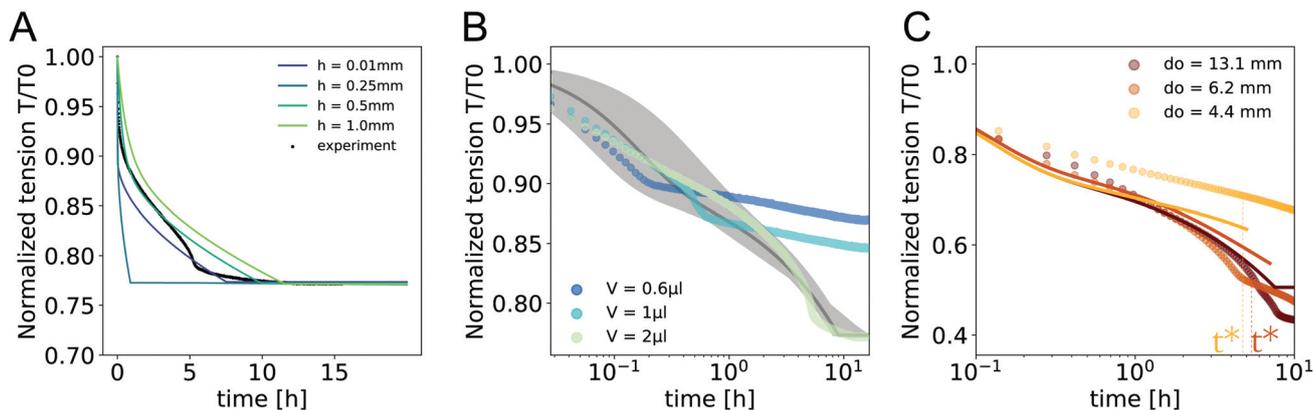
Fig. 3 Model calibration and results. (A) Experimental (black) and simulated tension in the fibre for various values of h with $D = 0.9 \times 10^{-10}$ m^2 s^{-1}. (B and C) Simulated values of T for experiments with 2 drops from Fig. 2 (eqn (8)) with h = 250 nm. The simulations are only plotted for times t to t*. The experimental values of t* are shown in the graph.

experiments although for small volumes, the model under-estimates the decrease in tension. For the two drop experiments, we can accurately reproduce the tension curves at short times (t to t*), as represented in Fig. 3C.

The comparison of the results of the model with the experiments is satisfactory with regards to the approximations made. In particular, it is not valid at short times when the diffusion is not 1D in the fibre. This might explain some differences at very short times. The fact that our model does not take the fluid release into account may explain some of the differences in the absorption dynamics at longer times in the two drops experiment. In addition, the drops are completely fixed in our modeling, even though they may become mobile in the experiment once deswelling occurs. The exact mechanisms behind droplet motion (e.g. differences in Laplace pressures) are beyond the scope of this study. The position of the drops defines the length over which the fluid has to diffuse and thus the speed of the absorption leading to differences between model and experiment.

In order to explain the deswelling observed in our experiment we consider the radius of the fibre. Indeed eqn (7) shows the dependence of the equilibrium concentration and thus of the radius (via eqn (3)) on the tension. The more the fibre is

stretched, the more it will be able to absorb solvent. We call R_{max} the radius that is reached at a given point where $c = c_{max}$. In our experiment, the tension is continuously decreasing leading to a decrease in $R_{max}(t)$ which is recovered in all simulations (Fig. 4). In Fig. 4A, we plot the normalized radius at the center $R_0 = R(z = 0)$ vs. time for the experiments of Fig. 2. As the liquid is absorbed, $R_0(t)$ increases while $R_{max}(t)$ decreases. For close drops ($d_0 r L_{swollen}$), R_0 overshoots the equilibrium radius (red line). In fact, this overshoot corresponds to the sudden detection of the expelled oil drop at the center. For large values of $d_0 4 L_{swollen}$, the radius remains smaller than the equilibrium radius and no deswelling is observed. Fig. 4B shows the predicted normalized radius at z = 0 and the predicted equilibrium radius (black curve) for distances ranging from 0.34 to 1.03 $L_{swollen}$. Also indicated are the times t_f at which all the fluid in the drops has been absorbed. t_f is almost constant for drops that are far apart but increases drastically below a critical value of d_0. This is due to the slowed down diffusion towards the center once it is filled with fluid. We can also note that R_0 increases faster for small distances since the fluid needs to travel a shorter distance and arrives faster. For small enough distances ($d_0 t 0.6d_0$), R_0 reaches the maximal radius before t_f leading to an overshoot
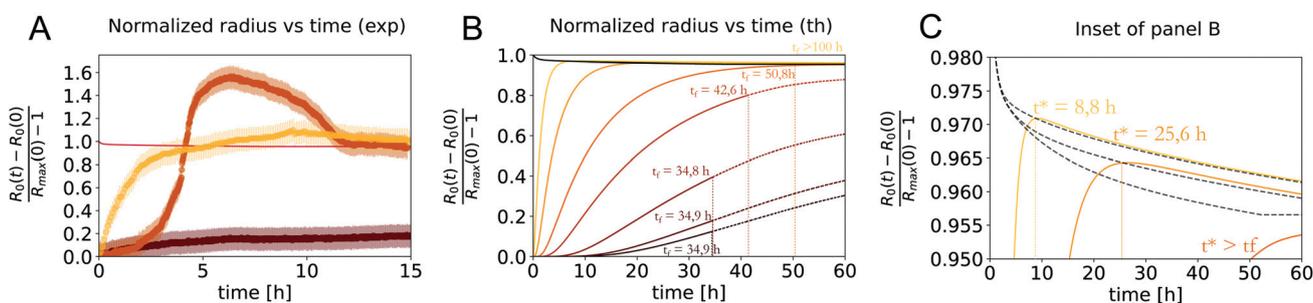

Fig. 4 Evolution of the fibre radius at z = 0. (A) Fibre radius at z = 0 for three experiments (V = 2 mL), $d_0/L_{swollen}$ = 1.126, 0.56, and 0.39 (dots). The continuous red line is the predicted value of the equilibrium radius $R_{max}(t)$. (B) Predicted normalized fibre radius at z = 0 for different values of $d_0/L_{swollen}$ (0.34, 0.43, 0.52, 0.6, 0.77, 0.94 and 1.03). The total absorption time denoted by t_f increases with time. (C) Inset of figure (B). Equilibrium radius (dashed) (eqn (7) and (3)) and centre radius (deduced from c) and eqn (3) for $d_0 = 0.34, 0.43$ and $0.52 L_{swollen}$. t* denotes the start of the overshoot corresponding to a saturation of the fibre at z = 0.

of the radius in the center over its equilibrium radius. This is clearer in Fig. 4C which is a closeup view of Fig. 4B. If the drops are too far apart, t^* would be reached after t_f which is impossible. When R_0 overshoots the maximal radius, there is an excess offluid at the center. In the experiment, we hypothesize that the most favourable way for the fluid to escape the center is localized deswelling, forming a new drop at $z = 0$. The model does not allow for fluid release outside of the fibre. Instead, the fluid needs to diffuse over a large distance (to the side of the drops) with a low concentration gradient. This process is slower than the decrease in maximal radius, prolonging the overshoot until all the fluid is absorbed.

We can also note that t^* is not reached at the same times, and therefore not at the same tension, for different distances (Fig. 4C). The length and intensity of the overshoot will change with the distance, which may lead to different expelled volumes.

3.2 Phase diagram

Fig. 5 presents the different possible outcomes when placing solvent drops of volume V on an elastomeric fibre at different distances d_0. We normalize the drop volume by the initial fibre volume $V_{f,0} = pR^2L_0$, and the distance by the swollen length $L_{swollen}$. We obtain three well separated regions in the phase diagram. For very small distances, the drops overlap at the start of the experiment and coalesce immediately (yellow diamonds, Fig. 5), before any swelling occurs. The condition for the drop to overlap can simply be written as $d_0 o l_{drop} (t = 0)$. For our range of volumes the length of a drop without gravity predicted by Carroll is satisfying. [8,9] At a given volume we recover the fact

that for drops that are far apart, no deswelling occurs (red circles, Fig. 5). For each drop volume, there is a critical value of d_0 below which there is enough volume in the drops to saturate the center and observe deswelling (empty green triangles in Fig. 5) possibly followed by drop movements and a complete coalescence (full triangles). As $L_{swollen}$ increases with V, this critical value of d_0 increases with the drop volume since more fluid is available and thus a larger portion of the fibre may be saturated with fluid. Experimentally, we detect deswelling if the drops are moving or if a third drop is clearly visible in the centre (i.e. $R_{measured} (z = 0) 4 1.1 R_0$). With our images, we are not able to detect a thin liquid film appearing at the surface of the fibres. Points gathered in a zone ofintermediate distances for large enough volumes correspond to deswelling cases.

A simple necessary condition for the deswelling is that the centre region between the two drops is saturated with fluid. Therefore, there has to be enough fluid inside the drop to account for the change in volume of the fibre portion between the two drops. In the case where the swelling is perfectly symmetrical around each drop, this separation criterion writes:

$$d_0 = L_{swollen} \qquad (9)$$

giving a minimal criterion for the deswelling. We plot the limit distance found with eqn (9) in Fig. 5 (red solid line). This criterion does not take into account the asymmetry of the diffusion once fluid arrives at $z = 0$ and the dependence on the tension of the swelling ratio. Indeed, the diffusion towards $z = 0$ is slower than the diffusion towards the fibre edges, and d_0 is necessarily smaller than the value given by this criterion. Our poroelastic model allows us to refine the separation criterion. Simulations are run for various initial volumes (from 0 to $0.5 V_f$) and distances (from 0 to 1.3 $L_{swollen}$) until the drops were fully absorbed by the fibre. Since the deswelling is caused by the decrease in tension after $t = t^*$ we plot the volume left in the drop at that time. This volume gives a quantitative indication of how much further the tension will decrease after t^*, before the drops are fully absorbed. If t^* is not reached before the drops are absorbed we fix $V(t^*) = 0$. This isocontour of $V(t^*) = 0$ is indicated by the dashed red line and indeed separates the experiments where deswelling is observed. The larger $V(t^*)$ is, the more the tension continues to decrease after t^*, thus possibly expelling more fluid from the fibre and increasing the possibility ofliquid motions and coalescences, as indeed observed experimentally.
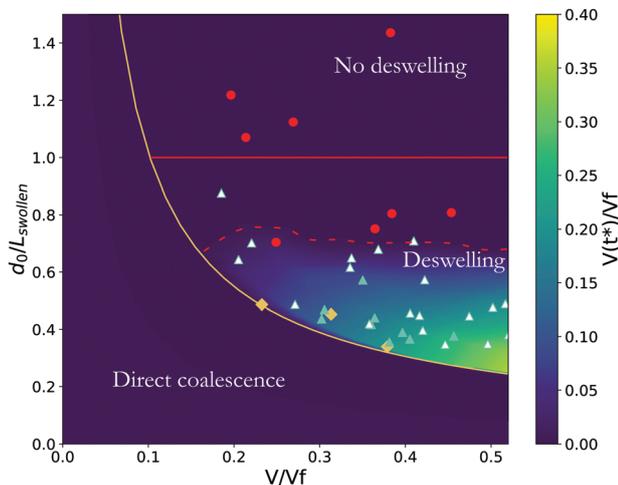

Fig. 5 Phase diagram after two drops of solvent swell an elastomer fibre. Outcome of the experiment for various drop volumes and initial distances d_0. V_f denotes the initial fibre volume. Red circles: the two drops never coalesce or interact. green triangles: deswelling is observed. filled triangles: full coalescence after deswelling occurs. yellow diamonds: immediate coalescence of the drops before any swelling occurs. The color-map presents the amount offluid remaining in the drops once saturation is reached (at $t = t^*$). The higher this volume is, the more likely we are to observe fluid deswelling. The red dashed line corresponds to isocontour of $V = 0$ separating the predicted regions of no deswelling and deswelling.

4 Discussion and conclusions

The coupling between constraints and thus stresses in a swelling (or shrinking) polymer has been investigated before. [22,24,26] In particular, the compression of the material caused by mechanical [24] or chemical constraints, [30–33] or sudden temperature changes [34] has been linked to fluid being released. This is often used in drug-delivery systems reacting to physio-chemical signals. When the solvent diffusion time within the polymer is comparable to the relaxation times of the polymer chains, [35] an

overshoot of the concentration over the final equilibrium value is observed, which is the sign that fluid is expelled during the swelling process.

By placing two drops of solvent on the fibre, we induce a non-homogeneous swelling of the material and show that a localized fluid release can occur spontaneously during swelling. Global constraints on the fibre geometry cause a compression of the material leading locally to an oversaturation of the elastomer and a spontaneous fluid release during the swelling process. We thus expect long range interactions, as any drop swelling the fibre will globally decrease its tension and may thus induce deswelling of saturated regions, even far away. This can be illustrated by the experiment shown in Movie S4 (ESI †) where we place several drops on the fibre. Initially, two drops are locally saturating the fibre but are slowly diffusing and not moving; adding several drops at different locations along the fibre, far from this region, leads to a global decrease of tension causing a local fluid release in the central saturated region, and induces the merging of the central drops. When considering fibre absorbing liquid from several isolated droplets instead of a bath we can thus expect complex fluid motions, including local transient fluid release, drop coalescence, and strong variations in absorption dynamics.

Author contributions

P. V., C. D. and S. P. designed research. P. V. performed experiments, J. D., P. V. Developed model, P. V., C. D., S. P., J. D. analyzed data, P. V., C. D., S. P., J. D. wrote paper.

Conflicts of interest

There are no conflicts to declare.

Notes and references

1 R. J. Roberts, PhD thesis, The Australian National University, 2004.
2 M. Parada, X. Zhou, D. Derome, R. M. Rossi and J. Carmeliet, Text. Res. J., 2019, 89, 3519–3528.
3 C. Duprat, Annu. Rev. Fluid Mech., 2022, 27.
4 C. Duprat and S. Protiere, EPL, 2015, 111, 56006.
5 J. Dervaux and M. B. Amar, Ann. Rev. Condens. Matter Phys., 2012, 24, 311–332.
6 D. P. Holmes, M. Roche´, T. Sinha and H. A. Stone, Soft Matter, 2011, 7, 5188–5193.
7 T. Bertrand, J. Peixinho, S. Mukhopadhyay and C. W. MacMinn, Phys. Rev. Appl., 2016, 6, 064010.
8 P. Van de Velde, S. Protie`re and C. Duprat, Soft Matter, 2021, 17, 6168–6175.
9 B. Carroll, J. Colloid Interface Sci., 1976, 57, 488–495.
10 E. Lorenceau and D. Que´ré, J. Fluid Mech., 2004, 510, 29–45.
11 D. P. Holmes, M. Roche´, T. Sinha and H. A. Stone, Soft Matter, 2011, 7, 5188.
12 A. Pandey and D. P. Holmes, Soft Matter, 2013, 9, 5524–5528.
13 A. Chakrabarti, G. P. Choi and L. Mahadevan, Phys. Rev. Lett., 2020, 124, 258002.
14 D. P. Holmes, P.-T. Brun, A. Pandey and S. Protie `re, Soft Matter, 2016, 12, 4886–4890.
15 P. J. Flory and J. Rehner, J. Chem. Phys., 1943, 11, 521–526.
16 S. A. Chester and L. Anand, J. Mech. Phys. Solids, 2010, 58, 1879–1906.
17 S. A. Chester and L. Anand, J. Mech. Phys. Solids, 2011, 59, 1978–2006.
18 T. Tanaka and D. J. Fillmore, J. Chem. Phys., 1979, 70, 1214–1218.
19 Y. Li and T. Tanaka, J. Chem. Phys., 1990, 92, 1365–1371.
20 M. Doi, J. Phys. Soc. Jpn., 2009, 78, 052001.
21 M. A. Biot, J. Appl. Phys., 1941, 12, 155–164.
22 T. Yamaue and M. Doi, J. Chem. Phys., 2005, 122, 084703.
23 W. Hong, X. Zhao, J. Zhou and Z. Suo, J. Mech. Phys. Solids, 2008, 56, 1779–1793.
24 K. Urayama and T. Takigawa, Soft Matter, 2012, 8, 8017.
25 C. J. Durning and K. N. Morman, J. Chem. Phys., 1993, 98, 4275–4293.
26 J. Yoon, S. Cai, Z. Suo and R. C. Hayward, Soft Matter, 2010, 6, 6004.
27 T. Hirotsu, Gels Handbook, Elsevier, 2001, vol. 1, pp. 65–97.
28 J. E. Mark, The Polymer Data Handbook, Oxford University Press, Oxford, New York, 2nd edn, 2009.
29 C.-Y. Hui and V. Muralidharan, J. Chem. Phys., 2005, 123, 154905.
30 G. W. Scherer, J. Non-Cryst. Solids, 1989, 108, 18–27.
31 G. W. Scherer, J. Non-Cryst. Solids, 1989, 108, 28–36.
32 M. Shibayama, M. Uesaka and Y. Shiwa, J. Chem. Phys., 1996, 105, 4350–4357.
33 S. Boral, A. Saxena and H. Bohidar, Int. J. Biol. Macromol., 2010, 46, 232–236.
34 R. Yoshida, K. Uchida, Y. Kaneko, K. Sakai, A. Kikuchi, Y. Sakurai and T. Okano, Nature, 1995, 374, 240–242.
35 W.-F. Lee and Y.-J. Chen, J. Appl. Polym. Sci., 2001, 81, 2888–2900.